Pure & Appl. Chem., Vol. 66, No. 6, pp. 1363–1372, 1994.
Printed in Great Britain.

Self consistent low pressure RF discharge modelling: comparisons with experiments in clean and dusty plasmas

Ph. Belenguer and J. P. Boeuf

Centre de Physique Atomique de Toulouse (CNRS URA 277), Université Paul Sabatier, 118, route de Narbonne, 31062 Toulouse CEDEX, France

Abstract: Self-consistent fluid and particle-in-cell Monte Carlo (PIC-MC) models have been used to study the electrical characteristics of rf discharges in clean and dusty plasmas. Numerical results in pure helium and silane and in dusty argon are compared with experimental measurements. The presence of large concentration of dust particles in the plasma modifies considerably the electrical characteristics of the discharge. The discharge impedance becomes much more resistive in presence of dust particles. Depending on the geometry of the reactor the appearance of electrostatic traps for negatively charged particulates has been studied with a 2D fluid model.

I. Introduction

Capacitively coupled radiofrequency discharges are routinely used in the microelectronics industry to produce plasmas for etching and deposition in semiconductor device fabrication. Discharge modelling has proved to be extremely useful to improve our understanding and interpretation of experiments.

The plasmas used in deposition or etching can generate solid particles whose size range from nanometers to micrometers. The formation of these particles depends on the physical and chemical characteristics of the discharge and is not well understood. They may be created in the gas volume by polymerisation of the gas or its dissociation products or ejected from the surface under plasma surface interaction. The formation and consequences of these particulates on the discharge has attracted recently the attention of researchers (1-6) because contamination of the substrate to be processed is a major concern in the micro electronics industry (7).

Dust particles in a weakly ionised plasma behave as electrostatic probes. Due to the large mobility of electrons compared with that of ions, the dust particles acquire a negative charge and a floating potential which is negative with respect to the plasma potential. The floating potential repels electrons and attracts ions and adjusts in such a way that at steady state, the flux of electrons to the dust particle is exactly compensated by the ion flux.

In section II, we present briefly the different self-consistent electrical models of the discharge. Results obtained in pristine helium and silane plasmas are presented in section III. In section IV, the influence of the presence of dust particles on the electrical characteristics of the discharge is analysed in the case of a dusty argon plasma and the results obtained by the models are compared to experimental measurements.

The role of the reactor geometry in the trapping of the dust particles is discussed with the help of a 2D fluid model of the discharge in section V.

II. Physical and numerical models

Self consistent numerical models have been used to describe the electrical characteristics of the discharges. A physical self consistent model of rf glow discharge must be based on equations describing electron and ion transport coupled with Poisson's equation for the electric field. As a first approximation we shall assume that the effect, on the charged particle kinetics, of the modification of the gas composition and temperature due to excitation, dissociation or heating can be neglected so that the charged particles interact with a cold, unchanging neutral background.

II.A. Fluid and particles models

Two different kinds of models have been used, fluid (1D and 2D) and 1D particle-in-cell Monte Carlo (PIC-MC) models. The 1D fluid model is a two electron group model. The bulk electrons are described by three moment equations, continuity, momentum (drift-diffusion approximation) and energy equation. Only the two first moments are considered for the ions. The electrons emitted by the electrodes and accelerated through the sheath are treated by a continuity and energy equation assuming a monoenergetic electron distribution. This model is based on the model described in ref. (8) where the local equilibrium hypothesis were assumed for the bulk electrons and ions. The results presented in silane and argon discharges have been obtained by the model assuming local equilibrium. This model has been modified to account for the presence of dust particles in dusty argon discharges (see ref. 6). To develop this model it was necessary to know the dust particle density (given by the experiment (6)), the number of negative charges carried by the dust and the electron loss frequency on the particulate. These data were provided by a 2D PIC-MC model described in ref. (5). The 2D fluid model is based on a three moment description of electron transport and a two moment representation of ion transport.

The PIC-MC model is based on a microscopic description of the electron and ion transport and is identical to the one used in Refs. (9,10). The trajectories of a sample of particles, electrons and ions are followed in velocity-position space. The equations of motion are integrated between collisions in a given electric field, and the field is recalculated using a Particle In Cell method (11) at short time intervals. Collisions (time, nature and scattering angle) are determined on the basis of random numbers generated according to probability density laws related to the charged particle-neutral cross-section, as in Monte Carlo simulations (12).

III. Pure helium and silane.

The aim of this section is to show that numerical models can reproduce correctly the electrical characteristics of the discharge and predict its behaviour when the operating conditions are modified. It is necessary to check the validity of these models in pristine plasmas prior the study of dusty rf discharges. We present results for rf discharges in pristine helium and silane plasmas.

III.A Helium discharges

It is now well known that rf discharges in helium can be sustained by different ionization mechanisms. Two discharge regimes referred as α and γ regimes have been studied numerically as well as experimentally (8,13-16). These denominations are related to the ionization mechanisms involved in

sustaining the discharge. Transition between these two regimes can be observed when the operating conditions of the discharge are modified.

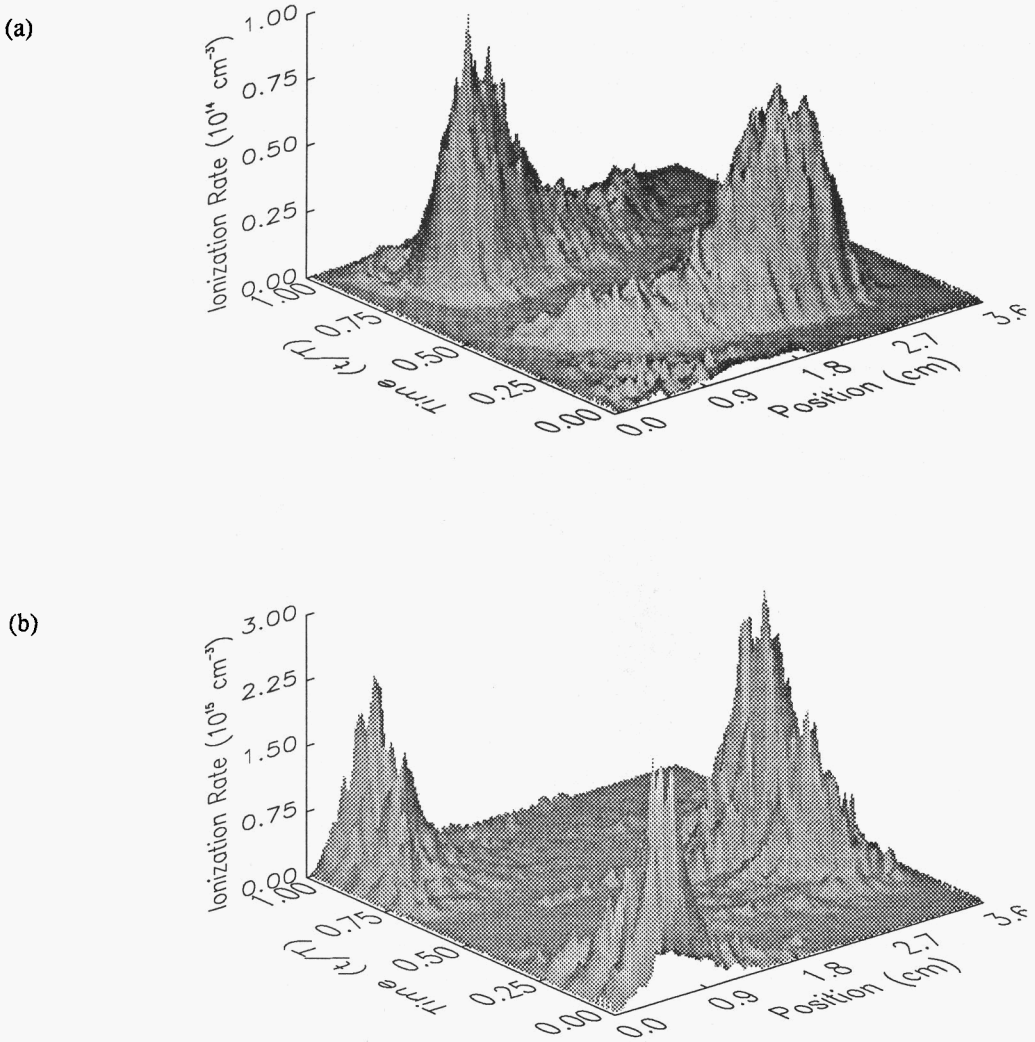

Fig. 1 Space and time variations of the ionization rate during a rf cycle for a 3.125 MHz discharge in helium, applied voltage 150 V (a), 370 V (b), gap length 3.6 cm, pressure 3 torr (PIC-MC model)

Figure 1 shows the ionization rate as a function of time and space in a 3.125 MHz discharge in helium at 3.0 torr and for an applied voltage of 150 V (Fig. 1a) and 370 V (Fig. 1b) obtained by a PIC-MC model. In the low voltage case, we can see two maxima in the ionization rate. These peaks correspond to the sheath expansion. We can see that there is no ionization during the sheath contraction. The ionization source is localised in the sheath or at the plasma sheath interface. This ionization mechanism is typical of radiofrequency discharges because it depends on the velocity of the sheath expansion and has been termed differently as "wave-riding", "Ohmic sheath heating", or "α regime". In the higher voltage case,

the peaks in the ionization rate occur at the time of maximum electric field and are present during the sheath contraction and expansion. The amplitude of the ionization peaks follows the amplitude of the electric field. We can note that the ionization is still important far away from the sheath regions. This ionization mechanism is similar to what appears in DC glow discharges where electrons emitted by the cathode are accelerated through the high electric field in the sheath and release their energy in the plasma. This regime is termed as "γ regime" according to the secondary electron emission coefficient γ. Under the operating conditions described below, a transition from the α regime to the γ regime will be observed when the voltage is increases from 150 V to 370 V. These results are in good qualitative agreement with the experimental measurements of Böhm and Perrin (17) of the He ($3^3D \rightarrow 2^3P^0$) 588 nm emission intensity. Furthermore, for higher voltage (470 V), they find a broad maximum of the emission at the center of the discharge. This maximum is mainly due to the built up of the He^* metastable density that affect the electron energy gain by superelastic collisions. Metastables are not taken into account in the model.

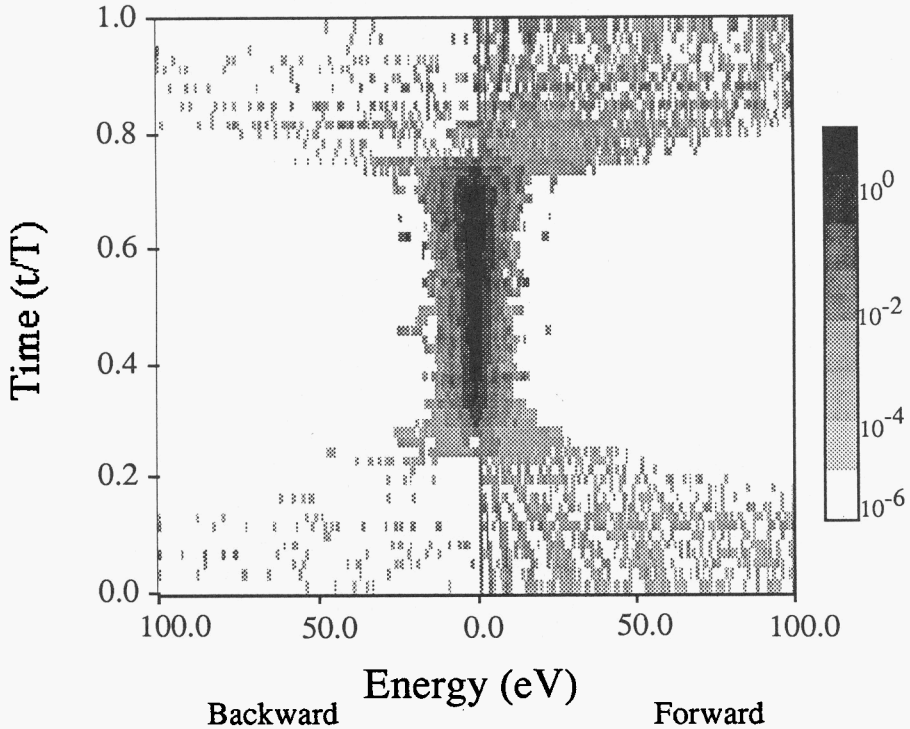

Fig. 2 Electron energy distribution function integrated between the abscissa 0.14 and 0.18 cm from the left electrode, as a function of energy and time during one rf cycle (conditions of Fig. 1), applied voltage 470 V. The distribution corresponding to electrons whose velocity is directed forward (toward the plasma center) or backward (toward the electrode) are represented separately.

Figure 2 shows the electron energy distribution function in the γ regime as a function of energy (in the forward and backward direction) and time during one rf cycle under the conditions of Fig 2. It is clear from this figure that the tail of the edf is strongly modulated with the applied voltage. The high energy tail is anisotropic with a large net velocity directed away from the electrode. The hypothesis of a forward directed beam in the fluid model is then quite realistic, even if the penetration depth of the beam may be overestimated.

III.B Silane discharges

Figure 3 shows the variations in space and time during one rf cycle of the ionization rate for a discharge in silane at 13.56 MHz, 30 mtorr for an electrode spacing of 3.6 cm and a peak rf voltage of 160 V. These conditions are similar to those used by Böhm and Perrin (18). The effect of secondary emission has been shown to be negligible under these conditions (9). We can see on this Figure that the ionization in the plasma volume is the main component of the total ionization and is modulated at twice the driving frequency. The electron losses by attachment have to be compensated by an increase in the ionization in the plasma which implies a high electric field in the bulk plasma. As in Fig. 2a, a distinct peak in the ionization rate is seen close to each electrode and during the sheath expansion. It is interesting to note also a lower peak in the ionization in front of the sheath during the anodic part of the cycle for the considered electrode. Similarly Flamm and Donnelly (19) have detected an increase of the light emission during the sheath contraction in chlorine discharge. This peak is seen in electronegative gases. In this case the plasma is dominated by negative and positive ions (electron density can be a hundred time lower). Near the electrode there is a net positive space charge that create a potential barrier for the electrons. The electrons are blocked until they acquire enough energy to pass this barrier and ionize when leaving the plasma (10, 20)

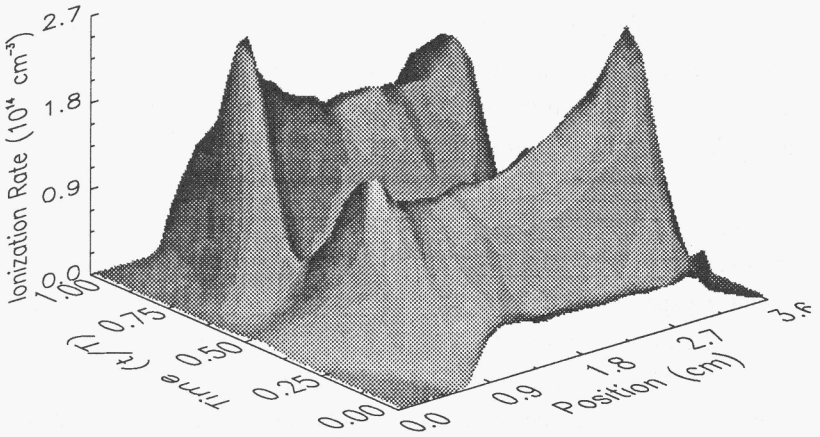

Fig. 3 Ionization as a function of space and time during one rf cycle for a discharge in silane, 30 mtorr at 300 K, gap length 3.6 cm, at 13.56 MHz, for an applied peak voltage of 160 V, (PIC-MC model).

Figure 4 shows the measured and calculated cosine of the current-voltage phase shift as a function of the peak rf voltage for the conditions of Fig. 3 at 0.055 torr (Fig. 4a) and 0.185 torr (Fig. 4b) at 200° C. In the low pressure case, the agreement between calculation and experiment is satisfactory. The observed discrepancy represents in fact only a few degrees. As can be expected for a frequency of 13.56 MHz, the discharge is mainly capacitive. The discharge is more capacitive when the voltage is increased because of the increase in the sheath field. For the higher pressure case the experimental results exhibit an abrupt transition in the discharge impedance. The discharge becomes much more resistive above 100-120 V. This transition can be reproduced by the model only if the attachment coefficient is artificially increased

by an order of magnitude. The role of this supplementary attachment is to introduce larger electron losses which must be balanced by an increase of ionization (electric field) in the plasma. The resistive component of the discharge impedance becomes more important. This increase in the electron losses in the plasma could be related to the appearance of powders when the power deposited in the discharge becomes important. This hypothesis can be supported by the hysteresis effect experimentally observed. Once created, the particulates are trapped in the plasma and do not disappear when the voltage is decreased.

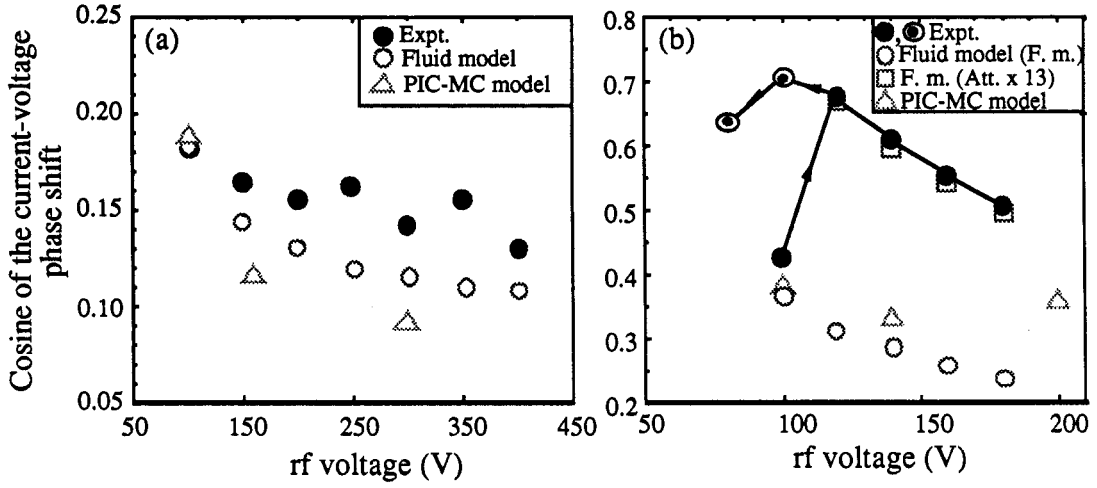

Fig. 4 Measured and calculated cosine of the current voltage phaseshift as a function of the peak rf voltage (measurements by Böhm and Perrin (18)): (a) 0.055 torr, (b) 0.185 torr at 200° C. The arrows indicate an hysteresis effect in the experiments.

IV.Clean and dusty argon discharges

A detailed description of the experimental set-up used to obtain the results presented in this section can be found in (6, 21). In the experiments the concentration and size of the dust particles were controlled and kept constant during the measurements. The particles were created in a silane-argon rf discharge and subsequently trapped in a rf discharge in pure argon. The silane being removed, the growth processes of the dust particles were therefore stopped and it was possible to measure the electrical characteristics of an argon plasma contaminated with dust particles of known density and size. Because of the large concentration of dust particles in the experiments it was necessary to take into account the space charge due to these particles in the numerical model. From the experimental measurements the size and concentration of dust particles are known. The experiments show that under the conditions considered, the dust particle concentration within the plasma is roughly spatially constant (the powders do not accumulate at the plasma sheath boundary as has been observed in other conditions). We have used a 2D PIC-MC simulation (5) to provide the floating potential and number of negative charges carried by the dust particle. This model provides the electron distribution function and hence the average frequency of electron loss on the dust particles. Knowing the dust particle density n_D and the number of negative charges Z_D and electron loss frequency ν_D, we can develop a complete model of a rf discharge in contaminated argon as follows. The charge density of dust particles is taken into account in Poisson's equation. In the conditions of the experiments this value, given by the 2D PIC-MC model is on the order of 30 for current densities in the mA/cm^2 range in agreement with the experimental measurements (22).

The profile of the distribution of dust particles in the plasma is obtained by assuming that they behave as heavy negative ions and by solving a continuity equation (drift-diffusion form) with no source term. The value of the dust particle density in the plasma center is taken equal to the experimental value (10^8 cm^{-3}). The density of negative charges corresponding to dust particles in the plasma center is therefore 3. 10^9 cm^{-3}. The electron and positive ion source terms in the corresponding continuity equations are modified to include the electron and ion losses on the dust particles. Under the conditions of the experiments, 0.11 torr argon, dust particle concentration 10^8 cm^{-3} and radius 0.05 μm, the 2D PIC-MC model gives $\nu_D \sim 3.10^6$ s^{-1}. The loss of electrons on the dust particle has to be compensated by an increase of the ionization in the plasma. This is made possible by an increase of the electric field in the plasma compared to a discharge in pure argon (the calculations gives 11V/cm instead of 1 V/cm).

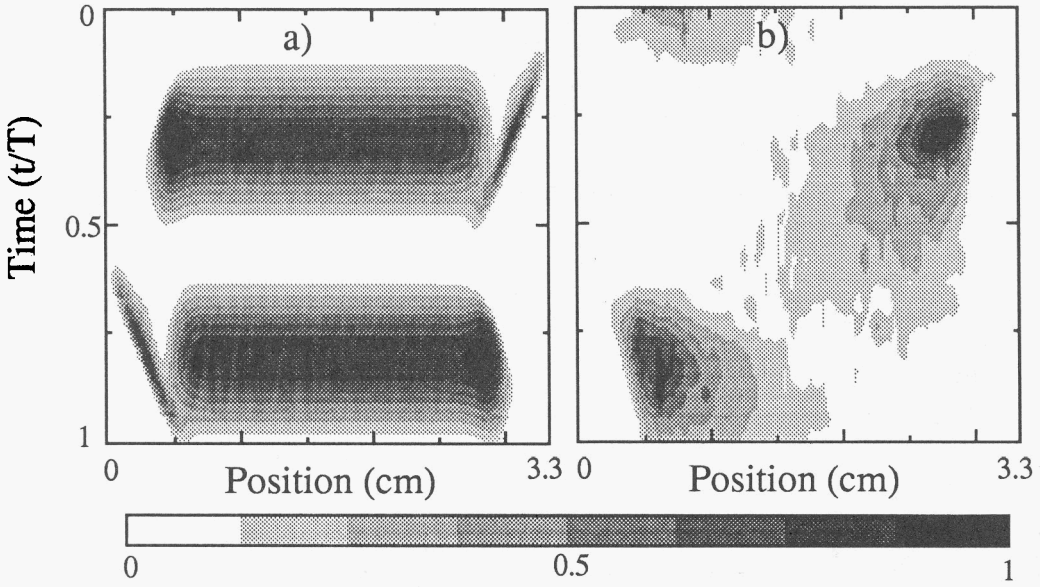

Fig. 5 Space and time variations of the ionization rate for a 13.56 MHz discharge in dusty (Fig. 5a) and pristine argon (Fig. 5b) at 0.11 torr, gap length 3.3 cm, peak rf voltage 200 V. Unit : a) $6.2x10^{15}$ cm^{-3} s^{-1}, b) $1.7x10^{15}$ cm^{-3} s^{-1}

This mechanism is clearly visible Fig. 5 which shows the space and time variations of the ionization rate in the case of dusty argon (Fig. 5a) and pure argon (Fig. 5b). The ionization mechanism in pure argon was mainly due to ohmic sheath heating as described in section III. In dusty plasma the ionization occurs mainly in the plasma and is modulated at twice the driving frequency. Under our conditions of large dust particle concentration, the discharge behaves as a discharge in an electronegative gas, the electron density is lower than the positive ions and negatively charged dust particles and the plasma is similar to a positive column plasma with a large sustaining electric field. To compare our results with experimental measurements the variations of the total current density as a function of the applied voltage is displayed Fig. 6. In dusty argon, the results obtained by the fluid model reproduce quite well the current obtained experimentally (Fig. 6a). It increases linearly as in the case of pure argon (Fig. 6b). Figure 7 shows the variations of the cosine of the current voltage phase shift for dusty and pristine argon. It appears that for the pure argon discharge (Fig 7b) and the dusty argon discharge (Fig 7a) the current voltage phase shift is very different. As described for the case of silane the presence of powder gives a resistive behaviour to

the discharge. This was expected since the presence of powders in the plasma induces a large increase in the plasma electric field.

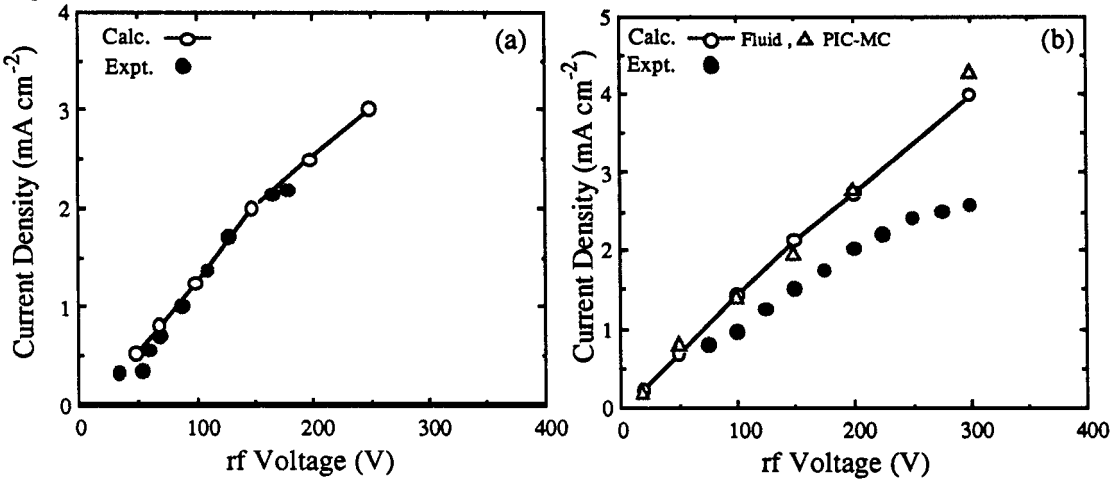

Fig. 6 Variations of the total current density as a function of the peak rf voltage. a) dusty argon, b) pristine argon. Same conditions as Fig. 5.

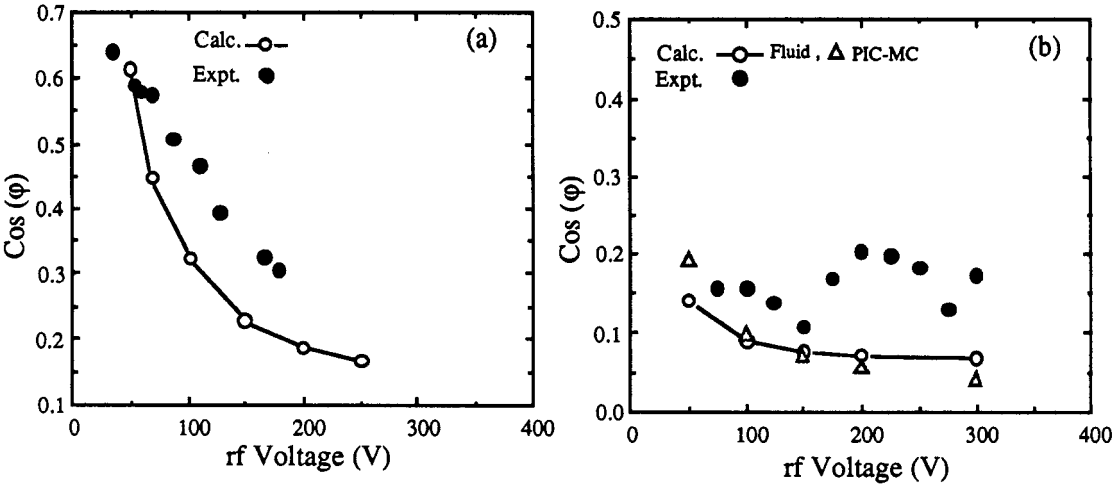

Fig. 7 Variations of the cosine of the current voltage phaseshift as a function of the peak rf voltage. a) dusty argon, b) pristine argon. Same conditions as Fig. 5.

V.Role of the reactor geometry in the negatively charged particle trapping

Under the conditions described previously the particulates were uniformly distributed in the plasma volume. It has been shown experimentally that dust particles can accumulate in some specific regions of the plasma and typically near the plasma sheath boundaries. The aim of this section is to show that the reactor geometry can induce electrostatic traps for the particulates that can explain their accumulation in well defined regions. Figure 8 presents the spatial distribution of the electron density (time averaged) in a 13.56 MHz discharge in 1 torr pure helium, 150 V peak rf voltage, for four different electrode configurations. The left electrode is powered through a capacitor and the right electrode is grounded. The calculated dc bias in each case is indicated on the figure. The averaged electron density presents maxima at different locations of the reactor chamber depending on the electrode geometry. In Fig. 8a, (symmetric

configuration) the region of maximum density are centered in the discharge and form a ring around the discharge gap; in this case, the walls of the discharge chamber are dielectrics. When the walls of the discharge are grounded, in the asymmetric conditions of Fig. 8b, the region of maximum density forms a ring around the left electrode. In Fig. 6c, we can see two regions of maximum density, one forming a ring around the left electrode and the other one forming a dome close the same electrode. In this case the wall of the chamber on the left electrode are also grounded. If the cylinder surrounding the left electrode is grounded, (Fig. 8d), we can see the maximum region of density forming the dome near the powered electrode but the ring has disappeared.

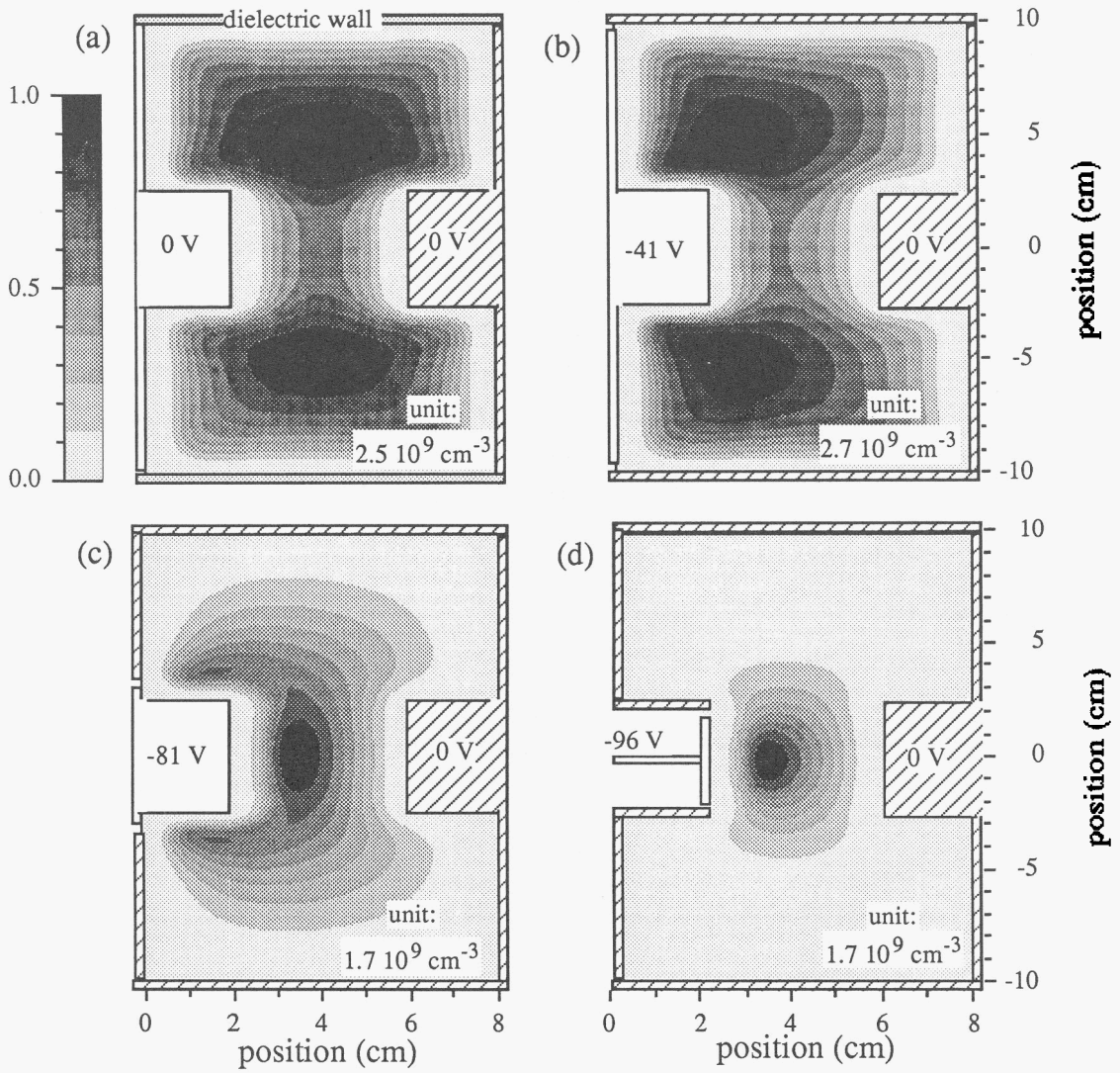

Fig. 8 Spatial distribution of the averaged electron density over a rf cycle, in a 13.56 MHz discharge in pure helium at 1 torr, applied peak rf voltage 150 V. The four case correspond to different electrode configurations. (a) dielectric walls, (b) grounded walls, (c) walls on the powered electrode also grounded, (d) cylinder surrounding the powered electrode also grounded.

The potential maxima are located at the same points as the density maxima. The maxima of plasma density are also strongly related to the spatial distribution of the ionization rate. These results are in

qualitative agreement with the light scattering measurements of Selwyn et al. (7). If the electrostatic forces are predominant,the maxima of the dust particle concentration will be located in the sam regions as the maxima of electron density, but with much larger peaks and gradients, due to the much smaller thermal energy of the dust particles.

References

1. T.J. Sommerer, M.S. Barnes, J.H. Keller, M.J. Mc Caughey and M.J. Kushner, Appl. Phys. Lett. **59**, 638 (1991)

2. M.J. Mc Caughey and M.J. Kushner, J. Appl. Phys. **69**, 6952 (1991)

3. M.S. Barnes, J.H. Keller, J.C. Forster, J.A. O'Neill, and D.K. Coultas, Phys. Rev. Lett. **68**, 313 (1992)

4. J.E. Daugherty, R.K. Porteous, M.D. Kilgore, and D.B. Graves, J. Appl. Phys. **72**, 3 (1992)

5. J.P. Boeuf, Phys. Rev. A **46**, 7910 (1992)

6. Ph. Belenguer, J.Ph. Blondeau, L. Boufendi, M. Toogood, A. Plain, A. Bouchoule, and C. Laure, Phys. Rev. A **46**, 7923 (1992)

7. S. Selwyn, J. Singh and R.S. Bennet, J. Vac. Sci. Tech. **A7**, 2758 (1989)

8. Ph. Belenguer and J. P. Boeuf, Phys. Rev. A **41**, 4447 (1990).

9. J.P. Boeuf and Ph. Belenguer, J. Appl. Phys. **71**, 4751 (1992)

10. L.C. Pitchford, Ph. Belenguer and J.P. Boeuf, in *Microwave Discharges: Fundamentals and Applications*, Edited by C.M Ferreira and M. Moisan, Plenum Press, New York, (1993).

11. C. K. Birdsall and A. B Langdon, *Plasma Physics via Computer Simulation*, Mc Graw Hill, New York, (1985)

12. J. P. Boeuf and E. Marode, J. Phys. D **15**, 2169 (1982).

13. S. M. Levitskii, Zh. Tekh. Fiz. **27**, 1001 (1957) [Sov. Phys. Tech. Phys. **2**, 887 (1958)]

14. N. A. Yatsenko, Zh. Tekh. Fiz. **50**, 2480 (1980) [Sov. Phys. Tech. Phys. **25**, 1454 (1980)]

15. V.A. Godyak and A. S. Kanneh, IEEE Trans. Plasma. Sci. **PS-14**, 112 (1986)

16. M. J. Kushner, IEEE Trans. Plasma. Sci. **PS-14**, 188 (1986)

17. C. Böhm and J. Perrin, Proceeding of the XX ICPIG, Pisa, Italy, (1991)

18. C. Böhm and J. Perrin, J. Phys. D: Appl. Phys. **24**, 865 (1991)

19. D.L. Flamm and V.M. Donnelly, J. Appl. Phys. **59**, 1052 (1986)

20. J.P. Boeuf and Ph. Belenguer, in *Non Equilibrium Processes in Partially Ionized Gases*, edited by M. Capitelli and J.N. Bardsley, Vol. 220 of Nato Advanced Study Institute, Series B: Physics, Plenum, New York, (1990)

21. A. Bouchoule, A. Plain, L. Boufendi, J. Ph. Blondeau and C. Laure, J. Appl. Phys. **79**, (1991).

22 L. Boufendi, A. Bouchoule, R.K. Porteous, J.P. Blondeau, A. Plain, and C. Laure, J. Appl. Phys., **73**, 2160, (1993)

Acknowledgements

This work has been supported by CNRS-PRSEM under contract N° 89N80/0095, and by the CNRS GRECO 57 "Interactions Plasmas Froids-Matériaux". The authors would like to thank A. Bouchoule, L. Boufendi, J.P. Blondeau, C. Böhm, and J. Perrin for a number of stimulating discussions.